Inflamm. Res. (2010) 59:531–541
DOI 10.1007/s00011-010-0157-9

Inflammation Research

ORIGINAL RESEARCH PAPER

Over-expression of caveolin-1 aggravate LPS-induced inflammatory response in AT-1 cells via up-regulation of cPLA2/p38 MAPK

Xue-Jun Lv · Yu-Ying Li · Yong-Juan Zhang · Mei Mao · Gui-Sheng Qian

Received: 4 September 2009 / Revised: 8 December 2009 / Accepted: 7 January 2010 / Published online: 23 January 2010

Abstract
Objective and design The aim of this study was to study the effect of caveolin-1 on the cytosolic phospholipase A2 (cPLA2), p38 mitogen-activated protein kinase (p38 MAPK) and nuclear factor κB (NF-κB) in mouse lung alveolar type-1 cells' (AT-1 cells) inflammatory response induced by LPS.
Materials and methods Gene clone technique was used to over-express caveolin-1 in AT-1 cells by lentivirus vector. The level of tumor necrosis factor α (TNF-α), interleukin 6 (IL-6), cPLA2, p38 MAPK and NF-κB was measured by ELISA, western blotting and EMSA.
Treatment AT-1 cells were treated with LPS.
Results Over-expression of caveolin-1 not only increased the production of pro-inflammatory cytokine TNF-α and IL-6, but also enhanced the expression of the cPLA2, p38 MAPK, and NF-κB.
Conclusions Our data demonstrated that over-expression of caveolin-1 aggravates the AT-1 injury induced by LPS, involving in modulation of the cPLA2 mediated by the cPLA2/p38 MAPK pathway.

Responsible Editor: G. Wallace.

X.-J. Lv and Y.-Y. Li contributed equally to this work.

X.-J. Lv · Y.-Y. Li · M. Mao · G.-S. Qian (✉)
Institute of Respiratory Disease, The Second Affiliated Hospital, Third Military Medical University, 400037 Chongqing, China
e-mail: ljdlxj@163.com

Y.-J. Zhang
Department of Physiology, Guangdong Medical College, 523808 Dongguan, China

Keywords Caveolin-1 · Cytosolic phospholipase A2 · Lipopolysaccharide · Nuclear factor κ B · p38 Mitogen-activated protein kinase

Introduction

Caveolae are omega-shaped invaginated membrane vesicular organelles with a diameter of 50–100 nm. Besides a distinctive lipid composition that is rich in glycosphingolipids, sphingomyelin, and cholesterol, the chief structure protein of caveolae are the caveolins [1]. Three caveolins have been identified: caveolin-1, caveolin-2, and caveolin-3. Caveolin-1 and -2 are usually co-expressed in many cell types such as endothelial cells and AT-1 cells; however, caveolin-3 is restricted to muscle cells. Caveolin-1, as a major resident scaffolding protein, participates in membrane trafficking and signal transduction [2–4]. Caveolin-1 also interacts with other signaling molecules and regulates their activation. Usually direct interaction of caveolin with signaling molecules leads to their inactivation [5]. For example, caveolin-1 has been reported to reduce cell growth and increase apoptosis by inhibiting activation of the growth factor receptor, downstream mitogen-activated protein kinase (MAPK) and the phosphatidylinositol 3 kinase (PI3 K) pathway [6–8].

Recently, it has been reported that detergent-insoluble caveolin-rich membrane domains are markedly enriched in phospholipase A2 (PLA2) and arachidonic acid, suggesting a possible role for PLA2 in caveolae-dependent cellular functions [9, 10].

PLA2s are a group of enzymes that catalyze the hydrolysis of sn-2 fatty acyl chain of phospholipids, and then produce lysophospholipids and free fatty acids such as arachidonic acid. Among PLA2s, the group IV 85 kD

cytosolic phospholipase A2 (cPLA2) is a pro-inflammatory enzyme found to be highly elevated in the circulation and local tissue, in association with a number of pathological conditions such as asthma and acute lung injury [11, 12]. Furthermore, a variety of pro-inflammatory stimuli such as cytokines and lipopolysaccharide (LPS) increase cPLA2 in many inflammatory cells [13]. The cPLA2 exhibits a preference for arachidonic acid in the sn-2 position in substrate phospholipids. Elevated levels of arachidonic acid are linked to a variety of metabolic and inflammatory diseases including lung inflammation [14]. Arachidonic acid acts directly as a second messenger or can be further metabolized to generate inflammatory mediators such as prostaglandins (PGs) [15]. PGs are ubiquitous compounds involved in a variety of homeostatic and inflammatory processes [16]. PGE2, one of the major PGs productions, exerts its biological effects by binding to specific cell surface receptors, designated PGE2 receptors (EPs). PGE2 is also involved in the activation of MAP kinases ERK and p38 MAPK [17]. On the other hand, p38 MAPK can regulate the activity of cPLA2 by direct phosphorylation [18]. The p38 MAPKs (four isoforms) are members of the MAPK family that are typically activated by environmental stresses and pro-inflammatory cytokines [19, 20]. p38 MAPK can regulate the expression and activity of nuclear transcription factors by direct phosphorylation, such as NF-κB and AP-1 [21].

In the present study, we increased specifically and transiently elevated caveolin-1 expression in AT-1 cells using gene clone technique and studied the effects of over-expression of caveolin-1 on cPLA2 and p38 MAPK and the consequent role in the AT-1 cells injury and in regulating pro-inflammatory cytokines synthesis, nuclear transcription factor activation following LPS challenge.

Materials and methods

Reagents

LPS (from E. coli 0111:B4), BAY11-7082, and SB203580 (the inhibitor of p38 MAPK) were purchased from Sigma (USA). ELISA kit for tumor necrosis factor-alpha (TNF-α) and IL-6 was purchased from Jingmei Chemical (China). The primary and secondary antibodies were purchased from Santa Cruz (USA). Methyl Arachidonyl Fluorophosphonate (MAFP) (the inhibitor of cPLA2) was purchased from MERCK (GEM), the FastStart DNA MasterPLUS SYBR Green I kit was purchased from Roche (GEM). All materials used in cell culture were certified as LPS free and tested by the Limulus amoebocyte lysate assay method to confirm the absence of detectable LPS.

Type I cells preparation and stimulation

AT-1 cells were isolated using several modifications of previously described methods for AT-1 and AT-2 cell isolation [22–25]. For each isolation, lungs from three male c57BL6 mice (20 g, the Third Military Medical University Breeding Laboratories) were perfused via the pulmonary artery with RPMI medium 1640 containing 25 mM *N*-2-hydroxyethylpiperazine-*N*′-2-ethanesulfonic acid (HEPES) (solution I) at 37°C. The lungs were lavaged via the trachea six times with Ca^{2+}, Mg^{2+}-free PBS containing 5 mM ethylenediaminetetraacetic acid (EDTA) and ethyleneglycoltetraacetic acid (EGTA) at 37°C and then were instilled with 5 ml of solution II (solution I with 10% dextran) containing elastase at 4.5 units/ml. The enzyme-instilled lungs were incubated at 37°C for 10 min; an additional 10 ml of the elastase solution was instilled continuously via the trachea over 30 min. After this enzymatic digestion, the trachea and large airways were dissected and discarded. The lung tissue was minced to 1 cubic mm fragments in solution II containing 20% fetal bovine serum and 50 μg of DNase/ml. The lung fragments were gently agitated by end-over-end rotation for 4 min and filtered once through 100 μm nylon mesh and then twice through 20 μm mesh. To further enrich for AT-1 cells, immunoselection was undertaken by incubating cells with the PE-labeled AT-1 cell-specific monoclonal antibody (MAb) RTI40 [26, 27], an integral membrane protein of type I cells for 30 min, according to the manufacturer's instructions. After being washed in RPMI 1640 with 1% FBS, cells were incubated with anti-PE magnetic beads for 15 min at 4°C. Bound AT-1 cells were selected by magnetic separation and re-suspended in RPMI 1640 with 1% FBS. Cell viability (>90%) was determined by trypan blue dye exclusion. Cell purity was determined by flow cytometry.

Lentivirus vector production and virus preparation

Recombinant lentivirus vector were packaged using a four-plasmid transient transfection procedure as described previously [28, 29]. The vector construct consists of a SV40-based lentivirus transfer vector expressing a green fluorescent protein (GFP) reporter gene driven by the cytomegalovirus (CMV) immediate-early promoter. Human 293T cells (80–90% confluence) were co-transfected by calcium phosphate precipitation with the 20 μg transfer vector, 10 μg pRsv-REV, 15 μg pMDlg-pRRE and 7.5 μg pMD2G plasmid. Virus was isolated and for some experiments was concentrated through a centrifugal concentrator and stored at −80°C. Titers of vector stocks were determined on HeLa cells by real-time PCR.

Cell line transduction and flow cytometry analysis

For transduction experiments, 1×10^6 cells were plated in each well of a six-well tissue culture treated plate. The following day, the medium was replaced with lentivirus (multiplicity of infection [MOI] of 5–50) and supplemented with 8 mg/ml of polybrene. The vector supernatant medium was replaced the following morning with fresh growth medium. The cells were passaged as needed and the proportion of cells expressing GFP was determined by flow cytometry 24 h later. For flow cytometry analysis of GFP transgene expression, cells were trypsinized, washed in PBS, and re-suspended in indicator-free Hanks' buffered saline. The samples were analyzed on a FACs Calibur using Cellquest software.

LPS challenge

AT-1 cells, either transfected with lentivirus vector as experiment group or empty vector (only encoding GFP) as control group, were treated with LPS at concentration 10 μg/ml at 2 and 4 h.

Cytokine assay

The level of cytokines (TNF-α, IL-6) released by LPS-stimulated AT-1 cells into the culture supernatant were measured by ELISA kits according to the manufacturer's instructions. The number of AT-1 cells was adjusted to 2×10^6 cells/ml with culture medium and treated or not treated with LPS as previously described. The cell suspension was transferred to the vials and centrifuged at 1500 rpm for 5 min. The supernatants were removed and the concentrations of cytokines in the supernatant were evaluated with ELISA assay kit.

RNA preparation and reverse transcription

RNA was prepared from samples following the TRIZOL protocol and finally suspended in an appropriate volume of RNAse-free water. 10 U of DNase I was added to remove traces of contaminating DNA. Approximately 1 μg of the preparation were mixed with a random primer, heated for 5 min to 55°C and cooled down on ice before adding 5 U of AMV-RT and 10 mM dNTPs in reaction buffer supplied by the manufacturer. Reverse transcription conditions were 60°C for 45 min, 95°C for 5 min, then cooled down on ice for 5 min.

Real-time PCR

Real-time PCR was performed on a Light Cycler using the FastStart DNA MasterPLUS SYBR Green I kit. For the amplifications of cPLA2 and p38 MAPK transcripts, the following primers were used for the analysis-cPLA2 F: 5′-TTATGTGTTTGATCGGGAAG-3′, cPLA2 R: 5′-CT CTCAACA ATGGCATCCTT-3′; p38 MAPK F: 5′-GAG CTGTTGACCGGAAGAAC-3′, p38 MAPK R: 5′-GG CTTGGCATCCTGTTAATG-3′. The amplification conditions were 95°C for 30 s and 45 cycles, each cycle at 95°C for 10 s, 55°C for 10 s and 72°C for 15 s. A standard curve covering a range of 10^3 copies to one copy was generated by primary isolating AT-1 cells in twofold serial dilutions. No template well without DNA was included as negative control. Each test sample was run in triplicate. The results were confirmed by gel electrophoresis (data not shown) and were analyzed using LightCycler software. The copy number was determined by the second derivative maximal analysis method.

Protein extracts

Extraction of cytoplasmic protein and nuclear protein are performed as previously described and according to the manufacturer's instruction [30–32].

AT-1 cells were homogenized in 200 μl of ice-cold cytoplasmic extraction reagent I (CER I) with protease inhibitor. At 10 min after incubation on ice, 22 μl of ice-cold cytoplasmic extraction reagent II (CER II) were added. At 1 min after incubation on ice, the homogenates were centrifuged at 16,000*g* for 5 min at 4°C. The supernatant was cytoplasmic protein. The pellets were washed with PBS and then the crude nuclear pellets were re-suspended in 100 μl of ice-cold nuclear extraction reagent (NER) with protease inhibitor and incubated on ice for 40 min. Nuclear extracts were recovered following centrifugation at 16,000 rpm for 10 min at 4°C, and then stored at −70°C.

Western blotting

The protein lysate-containing samples were subjected to electrophoresis on 6–15% polyacrylamide gel. Start wells were loaded with an equivalent amount of protein (25 μg/lane) or with the molecular weight markers. The separated proteins were electrotransferred from the gel to polyvinylidene difluoride (PVDF) membrane using the equipment for western blotting semi-dry apparatus. The membrane was incubated with the primary polyclonal antibody diluted at 1:1000 and then, with the secondary antibody at 1:500. The protein band was revealed by enhanced chemiluminescence. Integrated density value (IDV) was read using a densitometer.

Electrophoretic mobility shift assay (EMSA)

EMSA was performed as described previously [33]. Briefly, nuclear extract (5 μg) was incubated with 10 μl 2× binding buffer (10 mM Tris–HCl (pH 7.5), 50 mM

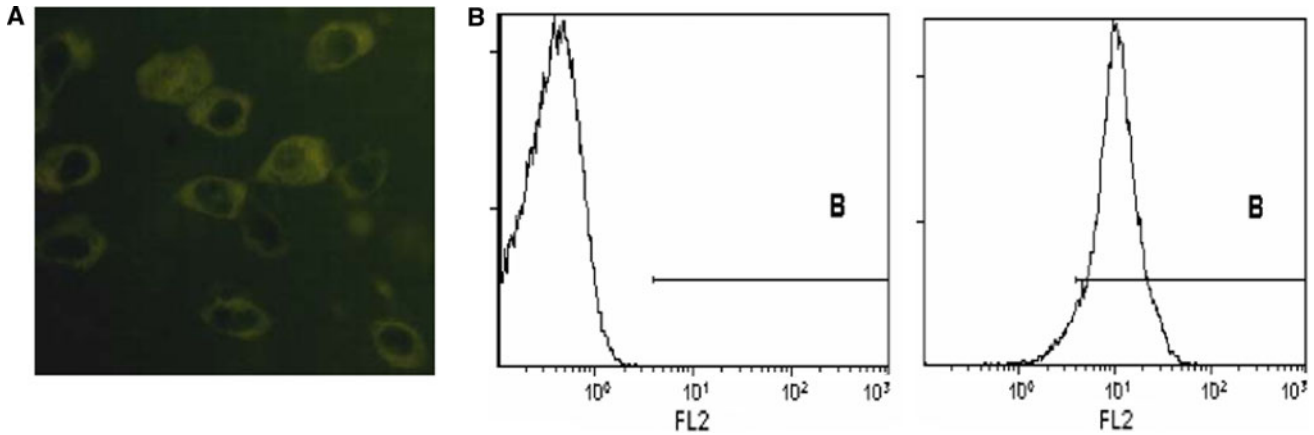

Fig. 1 Cytocentrifuged preparations of isolated cells were stained with PE-labeled anti-RTI40 Ab recognizing integral membrane proteins specific to AT-1 cells (Fig. 1a). To determine the purity of AT-1 cells, the isolated cells were analyzed by flow cytometry. Preparations containing <90% AT-1 cells were selected by magnetic separation again. The non-AT-1 cells included AT-2 cells and macrophages (Fig. 1b)

NaCl, 0.5 mM DTT, 10% glycerol and 1 μg of poly (dI:dC)) for 15 min at room temperature. Next, end-labeled double-stranded oligonucleotides (1 μl) containing the NF-κB site (10,000 cpm each) were added to the above reaction mixture and incubated at room temperature for 15 min. The sequence of the oligonucleotide was as follows: NF-κB, 5′-GATCATGGGGAATCCCCA-3′. For supershift assay, 2 μg of polyclonal anti-p65 antibodies were added, the mixtures were incubated at room temperature for 20 min. The labeled nuclear proteins were resolved by native PAGE using 0.5 × Tris/Borate/EDTA (TBE) buffer. The gel was then transferred to blotting paper and exposed to film at −80°C for 8 h.

Statistical analysis

Data are represented as mean ± SEM and analyzed by the Student's *t* test. All analyses were performed with SPSS 12.0.1 for Windows and were considered significant at $P < 0.05$.

Results

AT-1 cell preparations

The purity of type I cells in our cell preparations was assessed by flow cytometry with direct immunofluorescence (Fig. 1a). The percentage of type I cells ranged from 85 to 98%, with the major contaminants being type II cells and macrophages (Fig. 1b). Yields were 3–5 × 10^6 cells.

Lentivirus vectors achieve efficient transduction of AT-1 cells

Lentivirus transfer vector encoding the GFP marker gene was packaged by a standard four-plasmid cotransfection procedure. The titers of concentrated vector supernatants generated by this procedure are typically on the order of 2.5 × 10^8 TU/ml when titers were determined on HeLa cells. These vectors were used to transduce the AT-1 cells. Representative FACS analysis at 3 days post-transfection shows a shifted population of cells exhibiting higher fluorescence intensity specifically in the GFP wavelength (FL1 channel), with >95% GFP-positive cells, demonstrating that AT-1 cells are efficiently transduced by this vector (Fig. 2a, b). At 36 h post-transfection, caveolin-1 protein levels were significantly increased with the peak value at 72 h compared with that of the control, as evaluated by western blotting analysis (Fig. 2c).

Over-expressing caveolin-1 in AT-1 cells modulates LPS-induced cytokine production

To confirm whether caveolin-1 can modulate LPS-induced cytokine production, we used ELISA to detect cytokines TNF-α and IL-6 in the culture supernatant released by LPS-stimulated AT-1 cells. The results demonstrated that over-expression of caveolin-1 caused a significant increase in pro-inflammatory cytokines TNF-α and IL-6 at 2 and 4 h (Fig. 3a, b).

Modulation of the cPLA2 and p38 MAPK by caveolin-1

We attempted to delineate the possible mechanism of caveolin-1 on its inflammatory effects. We examined whether cPLA2 and p38 MAPK are modulated in caveolin-1 over-expressing AT-1 cells. The results showed that the mRNA expression of cPLA2 and p38 MAPK were significantly increased in caveolin-1 over-expressing cells at 2 and 4 h induced by LPS (Fig. 4a, b). The activation of the

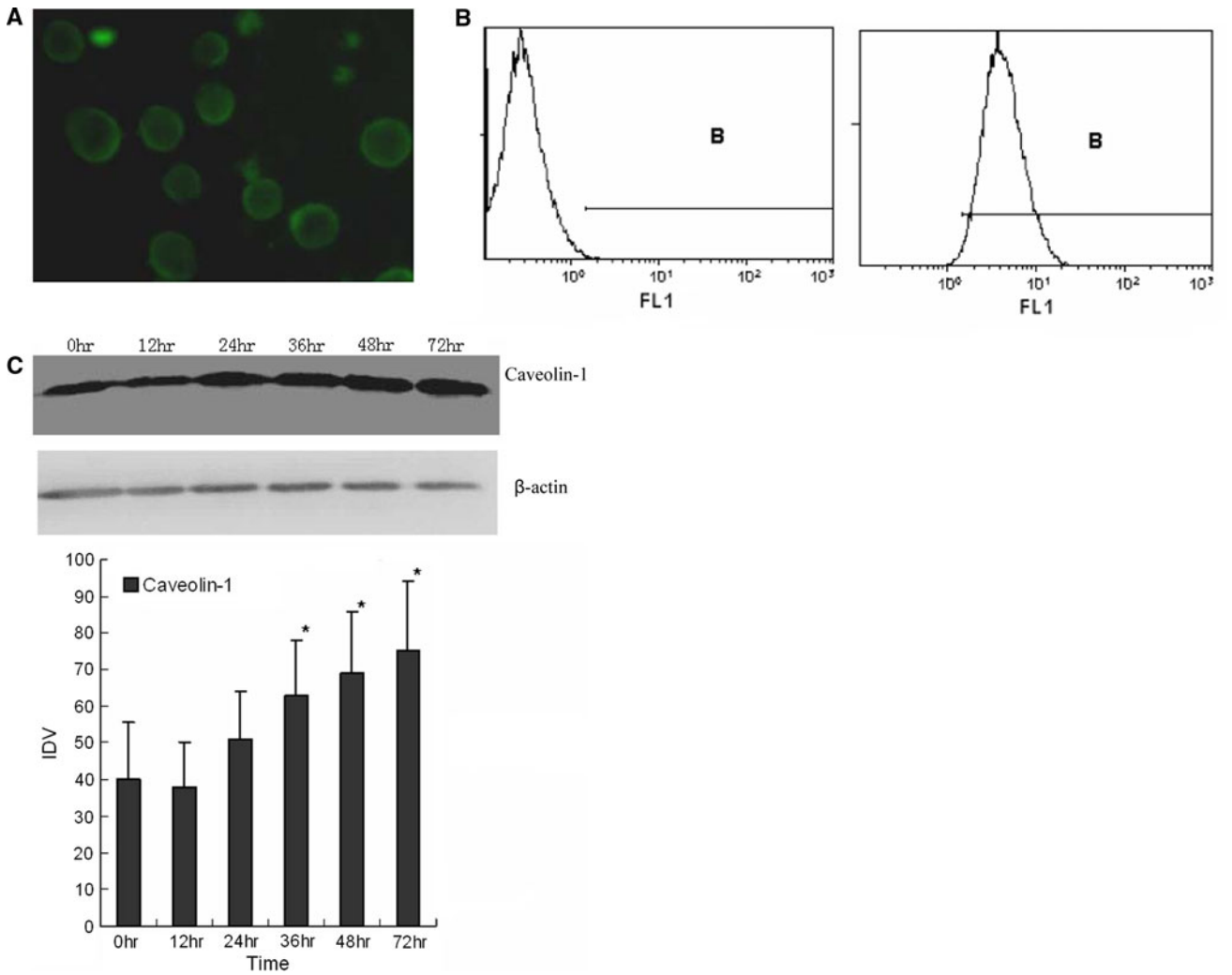

Fig. 2 Over-expression of the caveolin-1 in the AT-1 cells by lentivirus vector. The AT-1 cells grown on plastic tissue culture dishes were transfected with lentivirus vector (Fig. 2a). To determine the efficiency of transfection of lentivirus vector in AT-1 cells, the preparation cells were analyzed by flow cytometry. Representative FACS analysis at 72 h after infection demonstrates >95% GFP-positive cells at an MOI of 50 (Fig. 2b). The expression of caveolin-1 protein was evaluated at different times by western blotting. Caveolin-1 expression in cells increased in a time-dependent manner at 24 h post-transduction (Fig. 2c). $*P < 0.05$ compared with the production of caveolin-1 in the 0 h group

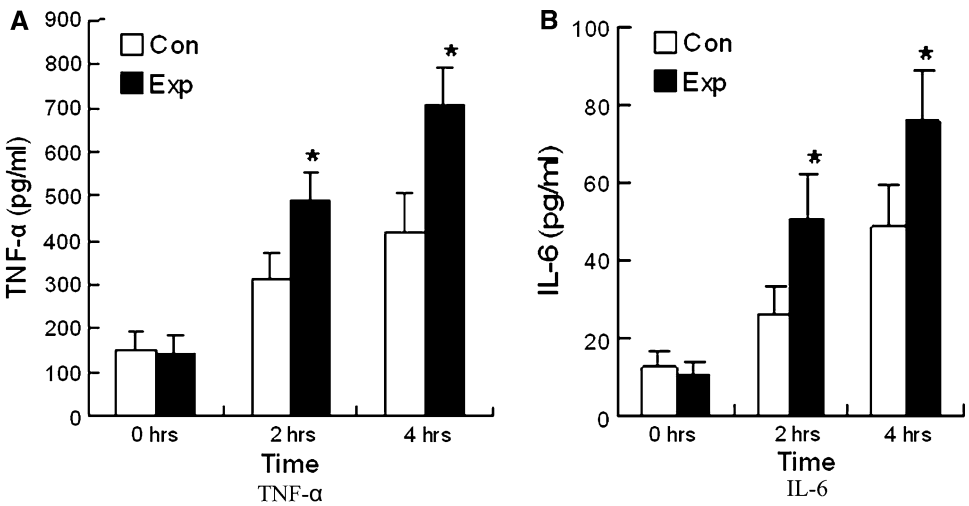

Fig. 3 Over-expressing caveolin-1 in AT-1 cells modulates LPS-induced cytokines production. AT-1 cells stably transfected with caveolin-1, were serum starved for 24 h and administered LPS for 2 and 4 h. The culture medium was harvested. TNF-α and IL-6 were determined by ELISA (Fig. 3a, b). $*P < 0.05$ compared with the control group

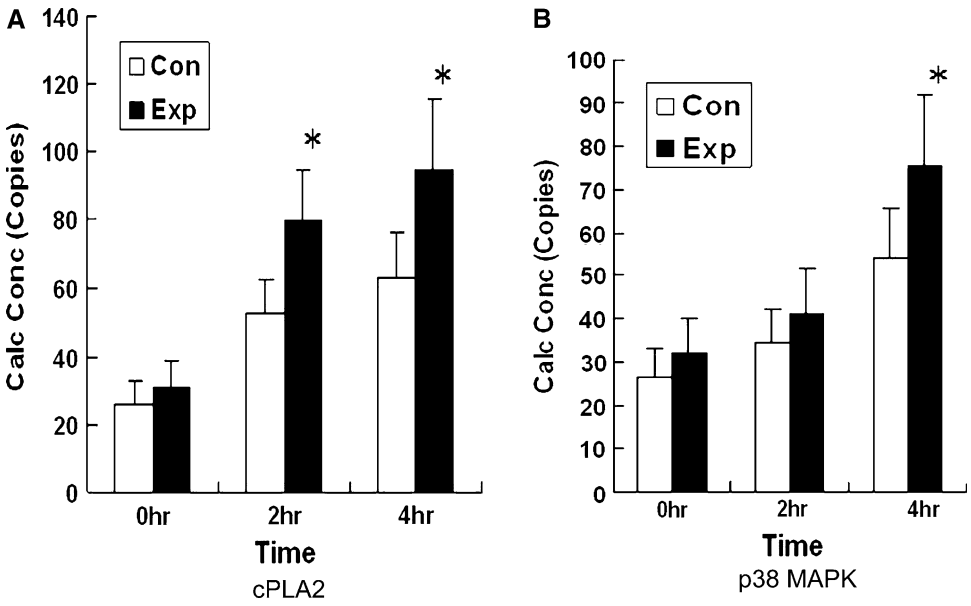

Fig. 4 Quantification of the mRNA of cPLA2 and p38 MAPK. After serum starvation for 24 h, AT-1 cells stably transfected with caveolin-1 were treated with or without LPS for 2 and 4 h. The cells were harvested and subjected to real-time PCR analysis for the cPLA2 and p38 MAPK expression at the mRNA level (Fig. 4a, b). $*P < 0.05$ compared with the control group

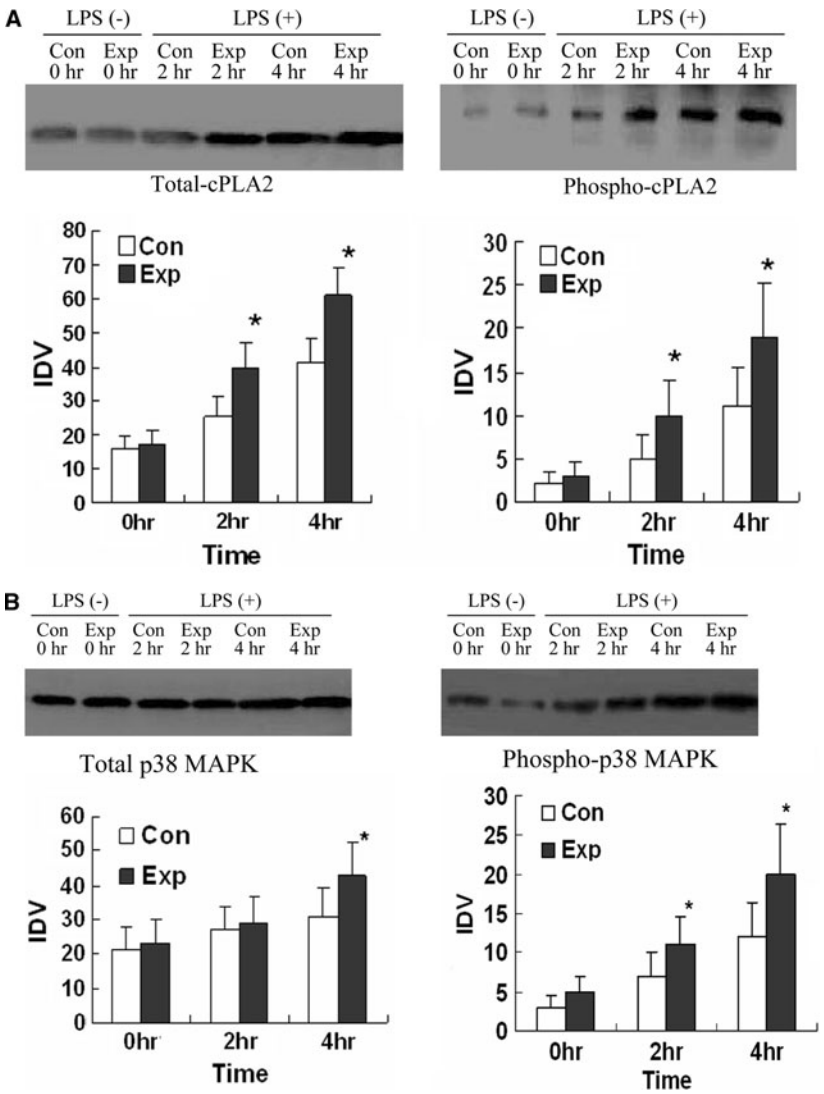

Fig. 5 Modulation of cPLA2 and p38 MAPK by caveolin-1. After serum starvation for 24 h, AT-1 cells stably transfected with caveolin-1 were treated with or without LPS for 2 and 4 h. The cells were harvested and subjected to western blotting analysis for total and phosphorylated cPLA2 (Fig. 5a) and p38 MAPK (Fig. 5b). $*P < 0.05$ compared with the control group

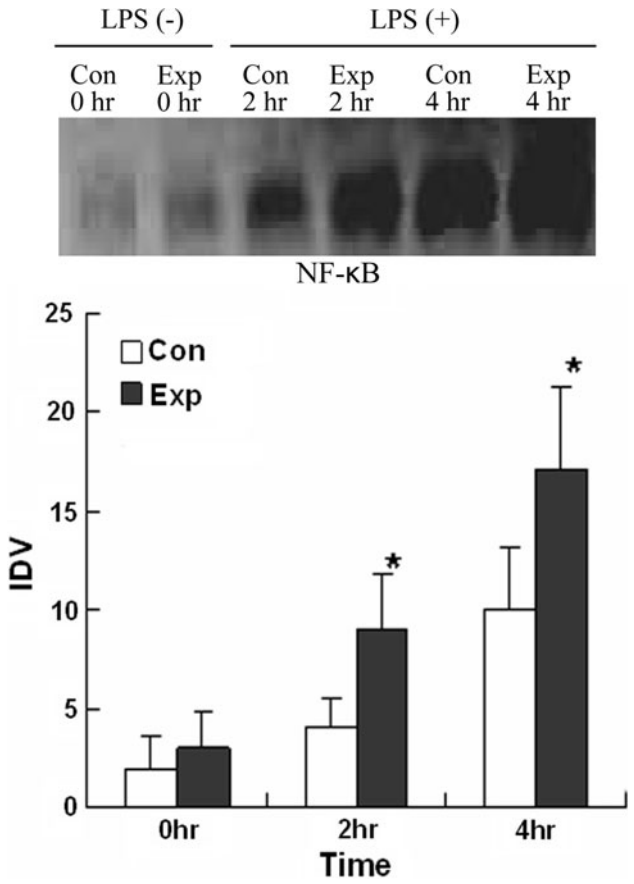

Fig. 6 Time course of LPS-induced NF-κB activation. NF-κB activity was measured by EMSA as described. Administration of LPS resulted in activation of NF-κB with peak activity occurring at 4 h (Fig. 6). *$P < 0.05$ compared with the control group

total and phosphorylated cPLA2 and p38 MAPK were significantly increased correspondingly. (Fig. 5a, b).

Modulation of the NF-κB by caveolin-1

The activation of NF-κB in the nucleus was estimated by EMSA. In the experimental group, the expression of NF-κB significantly increased in comparison to that in the control group (Fig. 6).

cPLA2 and p38 MAPK pathways are involved in the regulation of caveolin-1 on cytokine production

Because cPLA2 and p38 MAPK pathways were regulated by caveolin-1, we tested which pathway attenuation would lead to a loss of cytokine's modulation by caveolin-1. MAFP (the inhibitor of cPLA2), SB203580 (the inhibitor of p38 MAPK) and BAY11-7082 (the inhibitor of NF-κB) decreased TNF-α and IL-6 production compared with DMSO/LPS treatment. We observed significant differences in cytokine production (TNF-α and IL-6) between caveolin-1 over-expressing and control vector AT-1 cells in DMSO/LPS, MAFP/LPS, SB203580/LPS and BAY11-7082/LPS treatments (Fig. 7a, b). Then, we examined the interaction among the cPLA2, p38 MAPK, and NF-κB. The results showed that pre-treatment with MAFP reduced the activation of phosphorylated p38 MAPK and NF-κB, compared with vector control (DMSO) (Fig. 7c). When the SB203580 was administered to AT-1 cells, the phosphorylated cPLA2 and NF-κB were inhibited, whereas the phosphorylated cPLA2 and p38 MAPK were not affected when BAY11-7082 was added (Fig. 7d, e). The results indicated that cPLA2 and p38 MAPK pathways are involved in the regulation of caveolin-1 on cytokine production.

Discussion

Caveolin-1, first identified about one decade ago, was reported to have many biological functions, including the regulation of cholesterol homeostasis, membrane trafficking, signal transduction pathways, proliferation and apoptosis in a diversity of cell types [34]. Caveolin-1 can regulate membrane receptor signal transduction either by directly binding to the receptor, or binding to the downstream molecules, through interactions mediated by its scaffolding domain [35]. Caveolin-1 is believed to be a crucial negative regulator of signal transduction molecules and to inhibit the activity of most of its interacting partners. For example, caveolin-1 negatively regulates smooth muscle cell proliferation, and confers anti-inflammatory effects in murine macrophages via the MKK3/p38 MAPK pathway [36–38]. In addition, it is reported that caveolin-1 acts as the inhibitory regulator of endothelial NO synthase (eNOS) by sequestering the enzyme in the caveolae membrane [39–42]. On the contrary, it is reported that deletion of caveolin-1 protects against oxidative lung injury via up-regulation of heme oxygenase-1 [43]. Reports suggest a possible role for the interaction of caveolin and PLA2, which are markedly enriched in the detergent-insoluble caveolin-rich membrane domains [9, 10]. As is known that PLA2s are a growing family of enzymes with distinct substrate specificity, cofactor requirements, subcellular localization, and cellular function. It is reported that cPLA2, which is widely distributed in cells and is activated by submicromolar intracellular Ca^{2+} concentrations and is phosphorylated by activated p38 MAPK, plays a central role in the regulation of arachidonic acid released from membrane phospholipids and catalyzes the production of various metabolites [44, 45]. Several works have reported that the airway anaphylactic response and adult respiratory distress syndrome are markedly reduced in cPLA2 knockout mice compared with wild-type mice

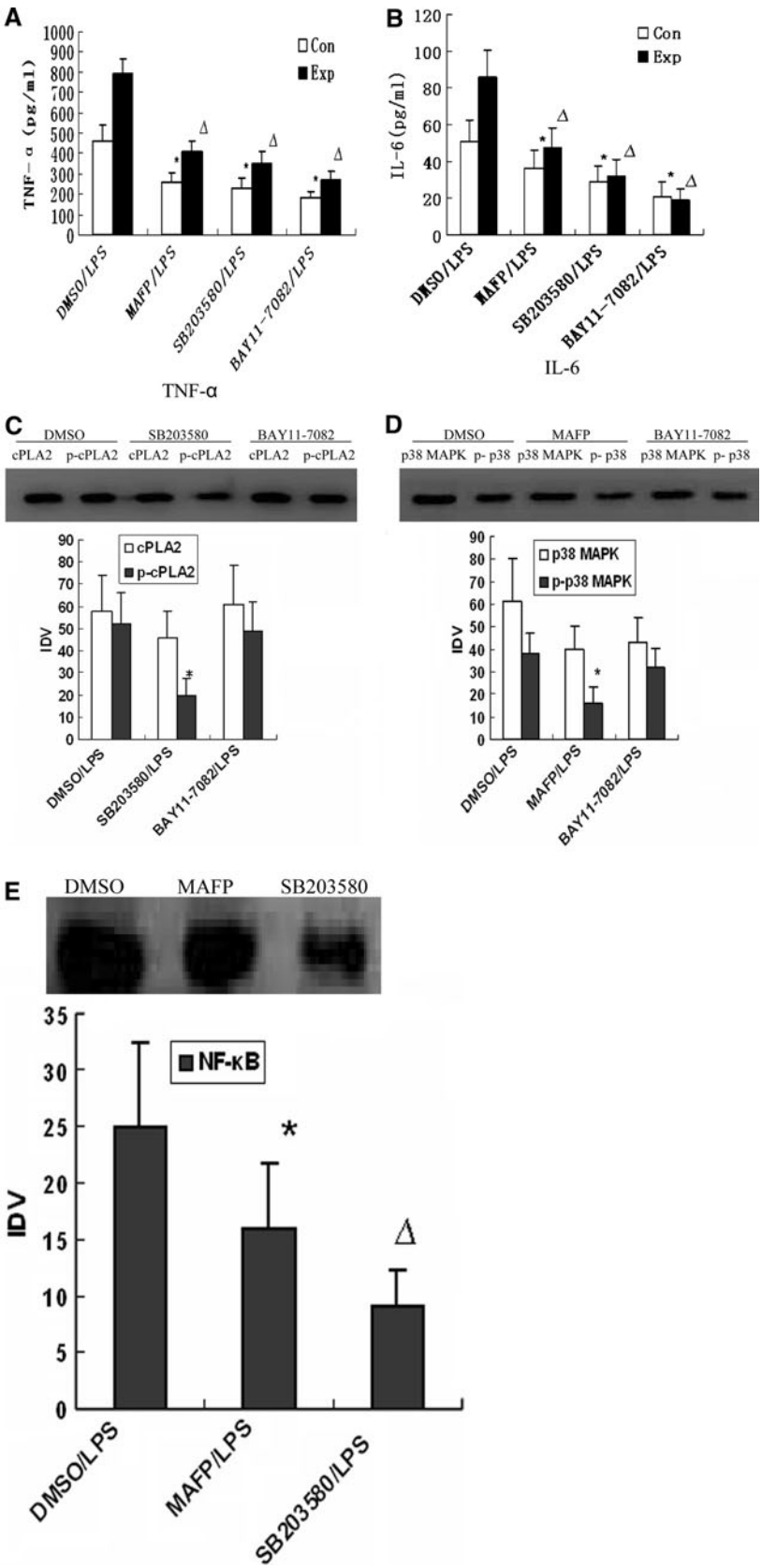

Fig. 7 cPLA2 and p38 MAPK pathways involved in the regulation of caveolin-1 on cytokines production. AT-1 cells stably transfected with the caveolin-1 gene and with the control vector were serum starved for 24 h. The cells were pretreated for 2 h with DMSO with or without different chemicals dissolved, including MAFP, SB203580 and BAY11-7082. The treated cells were then administrated LPS for 4 h. The culture media were harvested. Cytokine levels in culture medium were determined by ELISA (Fig. 7a, b). The cells were harvested and subjected to western blotting or EMSA analysis for total cPLA2, p38 MAPK and NF-Kb (Fig. 7c–e). $^{*}P < 0.05$ and $^{\Delta}P < 0.05$ compared with the DMSO/LPS

[46, 47]. Inhibition of cPLA2 prevented this response in wild-type mice with endotoxin-induced lung injury [48].

On the basis of these observations we initially hypothesized that caveolin-1 over-expressing AT-1 cells would be more resistant to LPS-induced injury. Surprisingly, and in contrast to our initial hypothesis, we found that caveolin-1 over-expressing AT-1 cells were susceptible to LPS-induced injury (Fig. 3).

We examined the underlying mechanisms by which the over-expression of caveolin-1 aggravate the injury in the AT-1 cells induced by LPS. Our data indicated that the apparent susceptiblity to LPS in the caveolin-1 over-expressing cells is due to increased activation of the cPLA2 and p38 MAPK (Fig. 4 and 5).

Recently, it is reported that cPLA2 and the metabolic products, such as arachidonic acid and PGE2, are involved in the pathogenesis of inflammation and are able to regulate gene expression through p38 MAPK signal transduction pathway and transcription factors such as NF-κB [49]. p38 MAPK signaling is critical for LPS-induced pulmonary inflammation, and is implicated in the initiation and evolution of LPS-mediated neutrophil accumulation in the acute lung injury [50]. For example, inhibition of p38 MAPK decreased neutrophil accumulation and IL-6 release in LPS-induced pulmonary inflammation [51]. Pulmonary inflammation can be reduced by administration of various p38 MAPK inhibitors before LPS challenge [50]. p38 MAPK signaling pathways have previously been implicated in the regulation of the NF-κB in response to diverse environmental stimuli [52]. We therefore hypothesized that the effect of caveolin-1 on p38 MAPK expression was related to caveolin-1 specific effects on cPLA2 gene activation and that the activated p38 MAPK could phosphorylate cPLA2. cPLA2 and p38 MAPK inhibitors blocked the effects of caveolin-1 on LPS-induced cytokines production. Thus, the interaction of cPLA2 and p38 MAPK aggravated the injury of AT-1 cells together with the downstream molecule (Fig. 7).

In this study, we also observed an increased NF-κB expression at an induced level (Fig. 6). NF-κB has well-known transcriptional factors that regulate LPS-induced cytokine production [53]. We explored the effects of caveolin-1 on NF-κB activation after LPS treatment. The results demonstrated that caveolin-1 markedly increased the activation as measured by EMSA. Given previous reports that p38 regulates NF-κB activation in macrophages [54], we hypothesized that p38 MAPK is involved in the up-regulation expression of NF-κB activation in AT-1 injury induced by LPS. It was illuminated further by the results of an NF-κB inhibitor blocking experiment .

In summary, these novel results demonstrate that the over-expression of caveolin-1 aggravates injury in the AT-1 cells by up-regulation of pro-inflammatory cytokine (TNF-α and IL-6) production. We have also presented evidence that the effect of caveolin-1 on the injury of AT-1 cells induced by LPS involves the cPLA2 and p38 MAPK signal pathway. We speculate that increased activation of cPLA2, p38 MAPK and downstream molecules lead to inflammation aggravation. We cannot exclude the possibility that the apparent LPS injury in AT-1 involves the activation or up-regulation of additional stress proteins, which warrants further investigation. In addition, our further directions will include studying the effect of caveolin-1 knockout on the cPLA2/p38 MAPK in vivo and in vitro. Taken together, caveolin-1 is an important mediator of inflammatory effects. These studies may provide additional therapeutic targets in the management or prevention of acute lung injury/acute respiratory distress syndrome.

Acknowledgments This work was supported by The National Natural Science Foundation of China (No. 3070346).

Conflict of interest statement None.

References

1. Rothberg KG, Heuser JE, Donzell WC, Ying YS, Glenney JR, Anderson RG. Caveolin, a protein component of caveolae membrane coats. Cell. 1992;68:673–82.
2. Scherer PE, Okamoto T, Chun M, Nishimoto I, Lodish HF, Lisanti MP. Identification, sequence, and expression of caveolin-2 defines a caveolin gene family. Proc Natl Acad Sci USA. 1996;93:131–5.
3. Scherer PE, Lewis RY, Volonte D, Engelman JA, Galbiati F, Couet J, et al. Cell-type and tissuespecific expression of caveolin-2: caveolins 1 and 2 co-localize and form a stable hetero-oligomeric complex in vivo. J Biol Chem. 1997;272:29337–46.
4. Tang Z, Scherer PE, Okamoto T, Song K, Chu C, et al. Molecular cloning of caveolin-3, a novel member of the caveolin gene family expressed predominantly in muscle. J Biol Chem. 1996;271:2255–61.
5. Li S, Okamoto T, Chun M, Sargiacomo M, Casanova JE, Hansen SH, et al. Evidence for a regulated interaction between heterotrimeric G proteins and caveolin. J Biol Chem. 1995;270:15693–701.
6. Mineo C, James GL, Smart EJ, Anderson RG. Localization of epidermal growth factor-stimulated Ras/Raf-1 interaction to caveolae membrane. J Biol Chem. 1996;271:11930–5.
7. Liu J, Oh P, Horner T, Rogers RA, Schnitzer JE. Organized endothelial cell surface signal transduction in caveolae distinct from glycosylphosphatidylinositol-anchored protein microdomains. J Biol Chem. 1997;272:7211–22.
8. Liu P, Ying Y, Ko YG, Anderson RG. Localization of platelet-derived growth factor-stimulated phosphorylation cascade to caveolae. J Biol Chem. 1996;271:10299–303.
9. Pike LJ, Han X, Chung KN, Gross RW. Lipid rafts are enriched in arachidonic acid and plasmenylethanolamine and their composition is independent of caveolin-1 expression: a quantitative electrospray ionization/mass spectrometric analysis. Biochemistry. 2002;41:2075–88.
10. Murakami M, Kambe T, Shimbara S, Yamamoto S, Kuwata H, Kudo I. Functional association of type IIA secretory

phospholipase A2 with the glycosylphosphatidylinositol-anchored heparan sulfate proteoglycan in the cyclooxygenase-2-mediated delayed prostanoid-biosynthetic pathway. J Biol Chem. 1999;274:29927–36.
11. Dennis EA. Diversity of group types, regulation, and function of phospholipase A2. J Biol Chem. 1994;269:13057–60.
12. Leslie CC. Properties and regulation of cytosolic phospholipase A2. J Biol Chem. 1997;272:16709–12.
13. Huber J, Fürnkranz A, Bochkov VN, Patricia MK, Lee H, Hedrick CC, et al. Specific monocyte adhesion to endothelial cells induced by oxidized phospholipids involves activation of cPLA2 and lipoxygenase. J Lipid Res. 2006;47:1054–62.
14. Qi HY, Shelhamer JH. Toll-like receptor 4 signaling regulates cytosolic phospholipase A2 activation and lipid generation in lipopolysaccharide-stimulated macrophages. J Biol Chem. 2005;280:38969–75.
15. Zhu X, Sano H, Kim KP, Sano A, Boetticher E, Munoz NM, et al. Role of mitogen-activated protein kinase-mediated cytosolic phospholipase A2 activation in arachidonic acid metabolism in human eosinophils. J Immunol. 2001;167:461–8.
16. Smith WL, DeWitt DL, Garavito RM. Cyclooxygenases: structural, cellular, and molecular biology. Annu Rev Biochem. 2000;69:145–82.
17. Ghayor C, Rey A, Caverzasio J. Prostaglandin-dependent activation of ERK mediates cell proliferation induced by transforming growth factor β in mouse osteoblastic cells. Bone. 2005;36:93–100.
18. Kramer RM, Roberts EF, Um SL, Borsch-Haubold AG, Watson SP, Fisher MJ, et al. p38 mitogen-activated protein kinase phosphorylates cytosolic phospholipase A2 (cPLA2) in thrombin-stimulated platelets. J Biol Chem. 1996;271:27723–9.
19. Herlaar E, Brown Z. p38 MAPK signalling cascades in inflammatory disease. Mol Med Today. 1999;5:439–47.
20. Karin M. The regulation of AP-1 activity by mitogen-activated protein kinases. J Biol Chem. 1995;270:16483–6.
21. Narayan RB, Douglas LF, Qin S, Aruna NB. p38 MAPK-mediated transcriptional activation of inducible nitric-oxide synthase in glial cells. J Biol Chem. 2002;277:29584–92.
22. Borok Z, Danto SI, Zabski SM, Crandall ED. Defined medium for primary culture de novo of adult rat alveolar epithelial cells. In Vitro Cell Dev Biol Anim. 1994;30A:99–104.
23. Borok Z, Hami A, Danto SI, Zabski SM, Crandall ED. Rat serum inhibits progression of alveolar epithelial cells toward the type I cell phenotype in vitro. Am J Respir Cell Mol Biol. 1995;12:50–5.
24. Dobbs LG. Isolation and culture of alveolar type II cells. Am J Physiol Lung Cell Mol Physiol. 1990;258:134–47.
25. Dobbs LG, Gonzalez R, Matthay MA, Carter EP, Allen L, Verkman AS. Highly water-permeable type I alveolar epithelial cells confer high water permeability between the airspace and vasculature in rat lung. Proc Natl Acad Sci USA. 1998;95:2991–6.
26. Dobbs LG, Williams MC, Gonzalez R. Monoclonal antibodies specific to apical surfaces of rat alveolar type I cells bind to surfaces of cultured, but not freshly isolated, type II cells. Biochim Biophys Acta. 1988;970:146–56.
27. McElroy MC, Pittet JF, Hashimoto S, Allen L, Wiener-Kronish JP, Dobbs LG. A type I cell-specific protein is a biochemical marker of epithelial injury in a rat model of pneumonia. Am J Physiol. 1995;268:181–6.
28. Naldini L, Blomer U, Gallay P, Ory D, Mulligan R, Gage FH, et al. In vivo gene delivery and stable transduction of nondividing cells by a lentiviral vector. Science. 1996;272:263–7.
29. Zufferey R, Nagy D, Mandel RJ, Naldini L, Trono D. Multiply attenuated lentiviral vector achieves efficient gene delivery in vivo. Nat Biotechnol. 1997;15:871–5.
30. Haddad JJ, Safi eh-Garabedian B, Saade NE, Lauterbach R. Inhibition of glutathione-related enzymes augments LPS-mediated cytokine biosynthesis: involvement of an IkappaB/NF-kappaB -sensitive pathway in the alveolar epithelium. Int Immunopharmacol. 2002;2:1567–83.
31. Carter AB, Monick MM, Hunninghake GW. Lipopolysaccharideinduced NF-kappa B activation and cytokine release in human alveolar macrophages is PKC-independent and TK- and PC-PLCdependent. Am J Respir Cell Mol Biol. 1998;18:384–91.
32. Richlin VA, Arevalo JM, Zack JA, Cole SW. Stress-induced enhancement of NF-kappa B DNA-binding in the peripheral blood leukocyte pool: effects of lymphocyte redistribution. Brain Behav Immun. 2004;18:231–7.
33. Skidgel RA, Gao XP, Brovkovych V, Rahman A, Jho D, Predescu S, et al. Nitric oxide stimulates macrophage inflammatory protein-2 expression in sepsis. J Immunol. 2002;169:2093–101.
34. Anderson RG. Caveolae: where incoming and outgoing messengers meet. Proc Natl Acad Sci USA. 1993;90:10909–13.
35. Pike LJ. Growth factor receptors, lipid rafts and caveolae: an evolving story. Biochim Biophys Acta. 2005;1746:260–73.
36. Kim HP, Wang X, Nakao A, Kim SI, Murase N, Choi ME, et al. Caveolin-1 expression by means of p38beta mitogenactivated protein kinase mediates the antiproliferative effect of carbon monoxide. Proc Natl Acad Sci USA. 2005;102:11319–24.
37. Peterson TE, Guicciardi ME, Gulati R, Kleppe LS, Mueske CS, Mookadam M, et al. Caveolin-1 can regulate vascular smooth muscle cell fate by switching platelet derived growth factor signaling from a proliferative to an apoptotic pathway. Arterioscler Thromb Vasc Biol. 2003;23:1521–7.
38. Wang XM, Kim HP, Song R, Choi AM. Caveolin-1 confers antiinflammatory effects in murine macrophages via the MKK3/p38 MAPK pathway. Am J Respir Cell Mol Biol. 2006;34:434–42.
39. Bernatchez PN, Bauer PM, Yu J, Prendergast JS, He P, Sessa WC. Dissecting the molecular control of endothelial NO synthase by caveolin-1 using cell-permeable peptides. Proc Natl Acad Sci USA. 2005;102:761–6.
40. Garcia-Cardena G, Martasek P, Masters BS, Skidd PM, Couet J, Li S, et al. Dissecting the interaction between nitric oxide synthase (NOS) and caveolin. Functional significance of the NOS caveolin binding domain in vivo. J Biol Chem. 1997;272:25437–40.
41. Michel JB, Feron O, Sacks D, Michel T. Reciprocal regulation of endothelial nitric-oxide synthase by Ca^{2+}-calmodulin and caveolin. J Biol Chem. 1997;272:15583–6.
42. Sessa WC. Regulation of endothelial derived nitric oxide in health and disease. Mem Inst Oswaldo Cruz. 2005;100 (Suppl 1): 15–8.
43. Jin Y, Kim HP, Chi M, Ifedigbo E, Ryter SW, Choi AM. Deletion of caveolin-1 protects against oxidative lung injury via up-regulation of heme oxygenase-1. Am J Respir Cell Mol Biol. 2008;39:171–9.
44. Borsch-Haubold AG, Kramer RM, Watson SP. Phosphorylation and activation of cytosolic phospholipase A2 by 38-kDa mitogen-activated protein kinase in collagen-stimulated human platelets. Eur J Biochem. 1997;245:751–9.
45. Borsch-Haubold AG, Bartoli F, Asselin J, Dudler T, Kramer RM, Apitz-Castro R, et al. Identification of the phosphorylation sites of cytosolic phospholipase A2 in agonist-stimulated human platelets and HeLa cells. J Biol Chem. 1998;273:4449–58.
46. Nagase T, Uozumi N, Ishii S, Kume K, Izumi T, Ouchi Y, et al. Acute lung injury by sepsis and acid aspiration: a key role for cytosolic phospholipase A2. Nat Immunol. 2000;1:42–6.
47. Miyahara T, Hamanaka K, Weber DS, Anghelescu M, Frost JR, King JA, et al. Cytosolic phospholipase A2 and arachidonic acid metabolites modulate ventilator-induced permeability increases in isolated mouse lungs. J Appl Physiol. 2008;104:354–62.

48. Nagase T, Uozumi N, Aoki-Nagase T, Terawaki K, Ishii S, Tomita T, et al. A potent inhibitor of cytosolic phospholipase A2, arachidonyl trifluoromethyl ketone, attenuates LPS-induced lung injury in mice. Am J Physiol Lung Cell Mol Physiol. 2003;284:720–6.
49. Wu T, Han C, Shelhamer JH. Involvement of p38 and p42/44 MAP kinases and protein kinase C in the interferon-γ and interleukin-1αinduced phosphorylation of 85-kDa cytosolic phospholipase A(2) in primary human bronchial epithelial cells. Cytokine. 2004;25:11–20.
50. Nick JA, Young SK, Arndt PG, Lieber JG, Suratt BT, Poch KR, et al. Selective suppression of neutrophil accumulation in ongoing pulmonary inflammation by systemic inhibition of p38 Mitogen-Activated Protein Kinase. J Immunol. 2002;169:5260–9.
51. Schnyder-Candrian S, Quesniaux VF, Padova FD, Maillet I, Noulin N, Couillin I, et al. Dual effects of p38 MAPK on TNF-dependent bronchoconstriction and TNF-independent neutrophil recruitment in lipopolysaccharide-induced acute respiratory distress syndrome. J Immunol. 2005;175:262–9.
52. Yang L, Zhu X, Tso MO. Role of NF-κB and MAPKs in Light-Induced Photoreceptor Apoptosis. Invest Ophthalmol Vis Sci. 2007;48:4766–76.
53. Lee JI, Burckart GJ. Nuclear Factor Kappa B: Important Transcription Factor and Therapeutic Target. J Clin Pharmacol. 1998;38:981–93.
54. Eswarappa SM, Pareek V, Chakravortty D. Role of actin cytoskeleton in LPS-induced NF-κB activation and nitric oxide production in murine macrophages. Innate Immun. 2008;14:309–18.